Chapter 5

Imaging through Graphene Templating

The contents presented in this chapter are based on Xu, K., Cao, P.G. and Heath, J.R. "Graphene visualizes the first water adlayers on mica at ambient conditions," *Science*, 329, 1188-1191 (2010) (Ref.[1]) and Cao, P.G., Xu, K., Varghese, J.O. and Heath, J.R. "Atomic force microscopy characterization of room-temperature adlayers of small organic molecules through graphene templating," *J Am Chem Soc*, 133, 2334-2337 (2011). (Ref.[2])

5.1 Introduction

In the previous chapter, we have described the electrical properties of graphene wrinkles and nanoribbons. Here we explore the application of graphene for imaging surface adlayers (for example, water) at ambient conditions. Under usual operating conditions, imaging of these dynamic adlayers through scanning probe microscopy is often prohibitively challenging because of the significant intervening force exerted by the probe tip. In our newly developed technique, graphene is used as an ultrathin (one atom thick) coating layer to fix the otherwise fragile surface adlayers, which enables characterization through atomic force microscopy (AFM) at room temperature.

5.1.1 Water

Water coats all hydrophilic surfaces under ambient conditions, and the first water adlayers on a solid often dominate the surface behavior.[3-6] Although scanning tunneling microscopy (STM) and other ultrahigh vacuum surface characterization techniques have

been extensively employed to study water (ice) adlayers on solids at cryogenic temperatures,[3, 4] such techniques are not applicable to room-temperature studies because of the high vapor pressure of water.[4, 5] Various optical methods have been used at ambient conditions to probe the averaged properties of water adlayers over macroscopic areas.[5, 7-9] Atomically resolved studies have remained challenging. For example, although thin ice layers have been studied with atomic force microscopy (AFM) below freezing temperatures,[10, 11] reliable AFM imaging of water adlayers under ambient conditions is confounded by tip-sample interactions.[4] For example, the capillary menisci formed between the tip and the sample strongly perturb the water adlayers on solids.[12]

Scanning polarization force microscopy (SPFM) has been utilized to image water adlayers.[4, 13, 14] For SPFM, the tip-sample distance is kept at tens of nanometers. By briefly contacting the tip on a mica surface to induce capillary condensation, metastable island-like structures were observed in SPFM images. These islands were interpreted as a second adlayer on a monolayer of water.[4, 14] However, the lateral resolution of SPFM is relatively low, and the measured apparent heights reflect local polarizability instead of actual heights. Furthermore, the structure of the *first* adlayer was not observed, likely because of the low lateral resolution and/or the dynamic nature of the first adlayer.[14]

In this chapter, we report on the use of monolayer graphene sheets as ultrathin coatings for enabling an AFM study of the first water adlayers on mica. Sputtered carbon is commonly used to coat biological systems, such as cells, for electron microscopy imaging. The carbon enables the imaging experiments by providing a protective (and conductive) coating. The graphene coating used here plays a somewhat similar role; graphene can tightly seal what are otherwise elusive adlayers, and stably "fix" the water

adlayer structures, thus permitting the detection of the structure of the first water adlayers under ambient conditions. Humidity-dependent experiments further reveal how the structure of the water adlayers evolves at the nanometer and molecular scale.

5.1.2 Organic molecules

The first layers of organic molecules adsorbed to solid surfaces often determine the physics and chemistry of both the adsorbate and the substrate, and thus play a crucial role in many applications, including, for example, heterogeneous catalysis, corrosion, adhesion, lubrication and environmental control.[15-17] For instance, the adsorption of volatile organic molecules on ambient surfaces plays an important role in determining the environmental fate of airborne organic pollutants.[16]

However, most of our current knowledge of adsorption processes has been gained from macroscopic measurements on large areas of surfaces, which provide limited information on the microscopic structures of adlayers. In particular, the structures of adlayers at the interfaces between solids and *vapors* of small organic molecules are poorly understood at ambient temperatures. The reasons are two-fold. First, organic compounds capable of forming vapors at room temperatures are inevitably volatile, and so molecularly thin adlayers on surfaces quickly evaporate away in the vacuum environments required by many surface characterization techniques. Second, when vacuum is not required, the microscopic structure of the adlayers is still difficult to probe due to the mobile nature of small molecules on surfaces, although certain area- and time-averaged properties can be determined (e.g., the averaged thickness of adlayers[18]).

As a result of these difficulties, previous experimental work on the room-temperature structures of weakly bound organic molecule adlayers (or molecularly thin

films) on solids has largely been limited to nonvolatile molecules (boiling point >>~250 °C) with high molecular weight (number of carbon atoms >>10).[19-25] Such adlayers (thin films) are typically obtained through coating from a solution phase, and so are fundamentally different from adlayers in equilibrium with a vapor. Alternatively, adlayers of small organic molecules have been studied at low temperatures (T<<200 K), where the vapor pressure and mobility of molecules are drastically reduced.[15, 17, 26, 27] However, the adlayer structures are found to be highly temperature-dependent,[17, 26] and thus the low-T results cannot be directly compared with the room-temperature vapor adsorption one encounters in everyday life.

In the remainder of this chapter, we report on the use of graphene sheets as an ultrathin coating/template for AFM characterization of the room-temperature structures of the adlayers at the interfaces between mica surfaces and vapors of small organic molecules. We show that graphene, albeit only one-atom thick, can prevent the evaporation of molecularly thin adlayers of volatile small organic molecules, and slows down, but doesn't fully prevent, the motions of the adsorbed molecules on the solid surface, thus allowing AFM observation of both the *structure* and *dynamics* of the adlayers at room temperature. Two common small organic molecules, tetrahydrofuran (THF) and cyclohexane, each representing one of the two classes of polar and non-polar organic solvents, were investigated and compared with water.

5.2 Experimental

5.2.1 Materials

Anhydrous inhibitor-free tetrahydrofuran (THF, ≥99.9%, water content <0.002%) and anhydrous cyclohexane (99.5%, water content <0.001%) were purchased from

Sigma-Aldrich. These reagents were used as supplied and stored in a glove-box purged with nitrogen. Muscovite mica (Grade V1; round disks of diameter 10 mm) was obtained from Ted Pella. Kish graphite was obtained from Covalent Materials US Inc.

5.2.2 Sample preparation

Single and few-layer graphene sheets were prepared by the standard method of mechanical exfoliation[28, 29] of Kish graphite on freshly cleaved muscovite mica. All experiments were performed at room temperature (22±2 °C). Humidity was monitored using a Fluke 971 temperature humidity meter. For graphene deposited on mica at ambient conditions, the ambient relative humidity (RH) was measured to be in a range of 36% to 42%. The low-humidity experiment was carried out in a glove-bag (Sigma-Aldrich AtmosBag) that was purged and protected under a continuous flow of ultrahigh purity argon. Mica disks were first heated in air at 200 °C for 10 min to remove any absorbed moisture, and then transferred into the glove-bag. The mica surface was cleaved in the glove-bag and allowed to equilibrate for ~5 min before graphene was deposited. A reading of RH = 1.8% to 2.1% was recorded for the process. The high-humidity experiment was carried out in a chamber with a beaker of water at the center. The mica surface was cleaved in the chamber and allowed to equilibrate for ~5 min before graphene was deposited. A reading of RH = 89±2% was recorded during the process.

For adsorption of organic molecules on mica, the mica was heated as mentioned above and transferred to the glove-bag in a low-humidity environment(<2%). The mica surface was cleaved in the glove-bag and exposed to organic vapors for ~10 s to ~1 min. The partial pressure of organic molecules at the mica surface, which determines the

surface coverage at equilibrium, was adjusted by varying the distance between the vapor source and the mica surface.

5.2.3 Identification of graphene layers

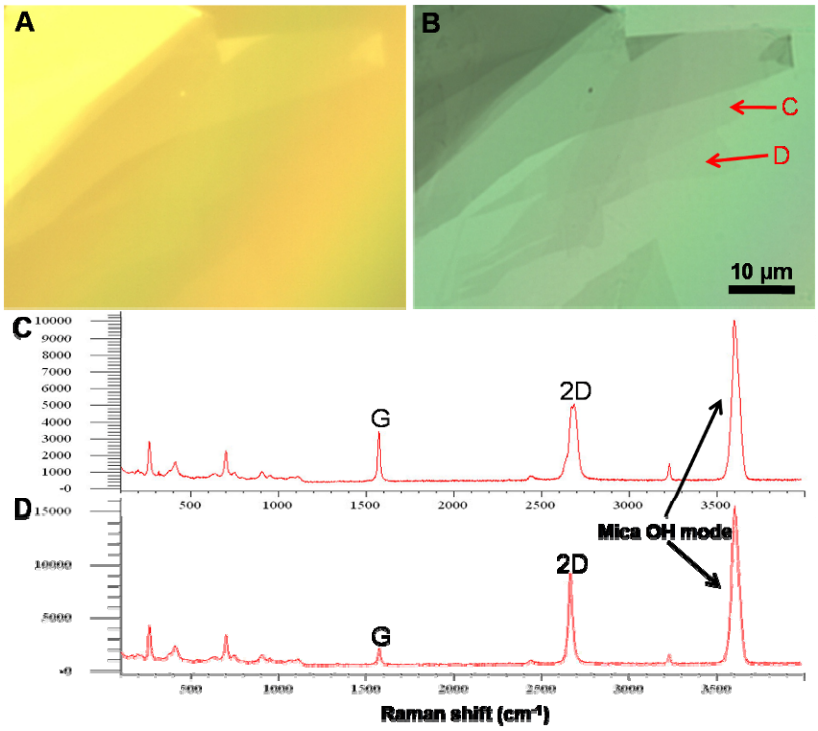

Figure 5.1. Few-layer graphene sheets are most readily observed through transmission optical microscopy. (**A**) In reflective optical microscopy, the thinnest graphene sheets are hard to see. (**B**) Transmission optical microscopy of the same area reveals the thinnest graphene sheets. (**C** and **D**) Raman spectra of two different regions of the graphene sheets as indicated in (B), corresponding to bilayer and monolayer graphene, respectively.

Graphene mono- and few-layers were identified through optical microscopy and confirmed by spatially resolved Raman spectroscopy. In the optical search process, we found it was easier to identify the thinnest graphene sheets using transmitted light (the

mica substrate is translucent and the graphene layers absorb white light[30]). Figure 5.1 A, B compares the optical images taken at reflection and transmission modes, respectively. The edges of the thinnest graphene layers are clearly resolved in the latter mode.

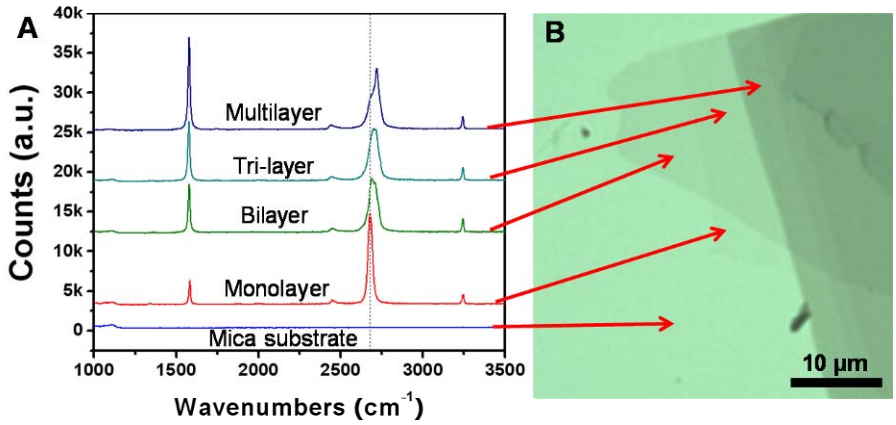

Figure 5.2. Identification of numbers of graphene layers in a representative sample. Spatially resolved Raman spectra of different regions in (**B**) are given in (**A**). Sample was made at ambient conditions.

Raman spectra were recorded with a Renishaw M1000 Micro Raman spectrometer system using a 514.5 nm laser beam and a 2400 lines per mm grating. A confocal optical microscope with a ×100 objective lens was used to record spectra with a spatial resolution of 2 μm. The numbers of grapheme layers were unambiguously confirmed through spatially resolved Raman spectroscopy.[31, 32] As shown in Figures 5.1 and 5.2, no noticeable D peak was observed in the Raman spectra of the deposited graphene, which is suggestive of high-crystalline order of our samples. The sizes of the identified graphene mono- and few-layers range from tens of micrometers to more than 100 micrometers.

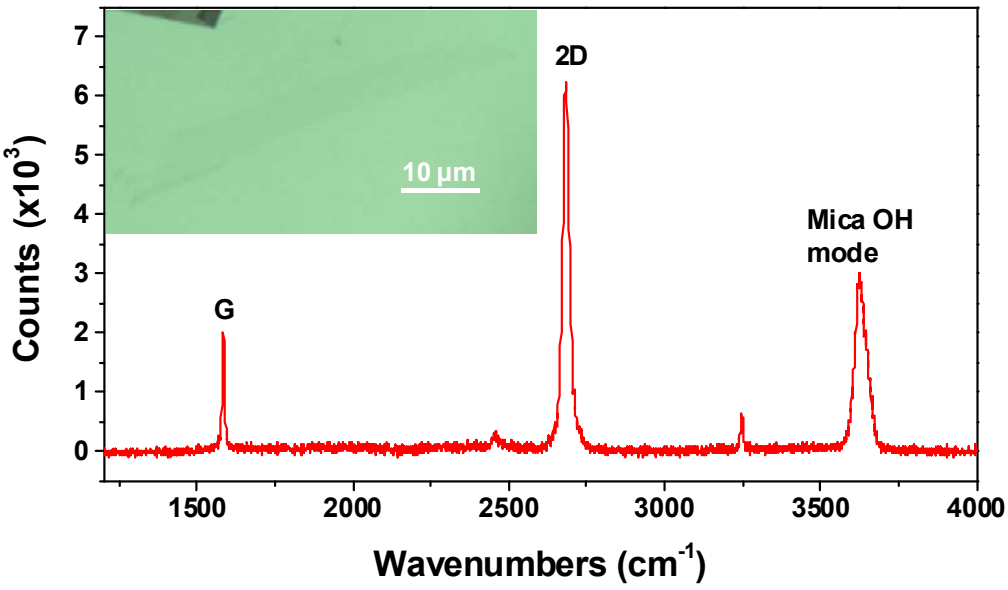

Figure 5.3. Raman spectrum of a monolayer graphene sheet deposited on a mica surface that was in equilibrium with a THF vapor. Inset: transmission optical image of the graphene sheet at the center. The 2D and G bands of graphene and the OH mode of mica are labeled. Similar Raman spectra were also observed for monolayer graphene sheets deposited on mica surfaces that were in equilibrium with cyclohexane vapors.

The layers of graphene for small organic molecules were identified in the same way as above and a typical spectrum for single-layer on THF adsorbed mica is presented in Figure 5.3.

5.2.4 Atomic force microscopy

All AFM images were acquired under tapping mode on a Digital Instrument Nanoscope IIIA at ambient conditions. A sharp TESP tip (Veeco) with a radius of end of 8 nm was used. Typical values for the force constant and resonance frequency were 42 N/m and 320 kHz, respectively. Height calibrations were performed using the step heights of freshly cleaved graphite samples. Due to the super-flatness of the samples,

sometimes the laser interference pattern along the slow-scan axis was hard to avoid, which is more noticeable in large-area scanning and has a period of twice the wavelength of the laser. This is caused by the constructive interference of laser reflected from the sample surface and that reflected from the cantilever. The broad stripe-like features seen in Figure 5.12ab were due to this effect.

5.3 Water on mica

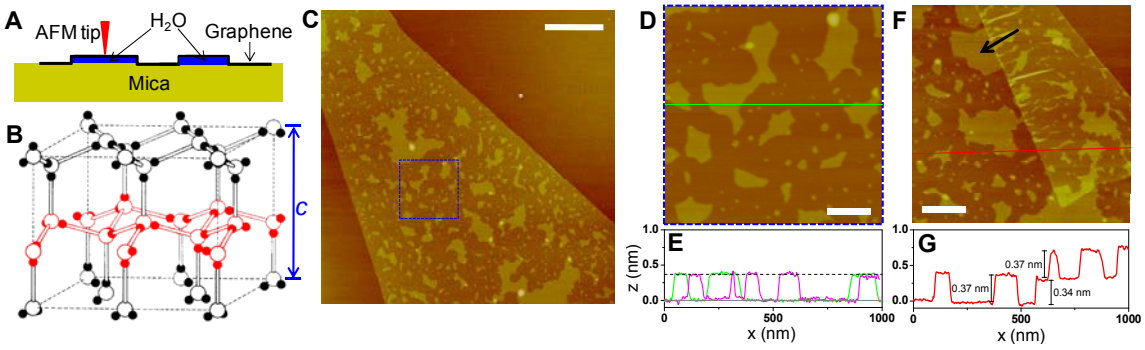

Figure 5.4. Graphene visualizes the first water adlayer on mica surface at ambient conditions. (**A**) A schematic of how graphene locks the first water adlayer on mica into fixed patterns, and severs as an ultrathin coating for AFM. (**B**) The structure of ordinary ice (ice I_h). Open balls represent O atoms, and smaller, solid balls represent H atoms. A single "puckered bilayer" is highlighted with red. Inter-layer distance is $c/2$ = 0.369 nm when close to 0 °C. Adapted from (Ref.[33]). (**C**) AFM image of a monolayer graphene sheet deposited on mica at ambient conditions. (**D**) A close-up of the blue square in (C). (**E**) Height profiles along the green line in (D) and from a different sample (Figure 5.6A). The dashed line indicates z = 0.37 nm. (**F**) AFM image of another sample, where the edge of a monolayer graphene sheet is folded underneath itself. Arrow points to an island with multiple 120° corners. (**G**) The height profile along the red line in (F), crossing the folded region. Scale bars: 1 μm for (C) and 200 nm for (D)(F). The same height scale (4 nm) is used for all images.

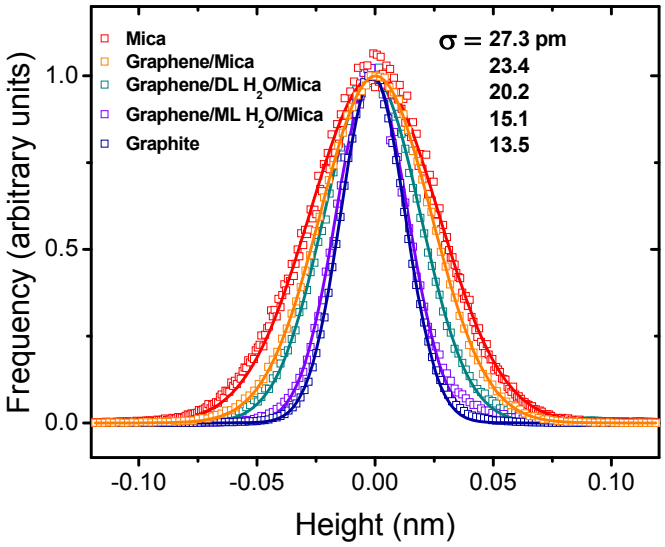

Figure 5.5. Comparison of the roughness of different surfaces. Height histograms (open squares) are given for a freshly cleaved mica surface, graphene on bare mica surface (from a sample prepared at 2% RH), graphene on a single water adlayer on mica (labeled as ML H_2O; from a sample prepared at 90% RH), graphene on top of two water adlayers (labeled as DL H_2O; from a sample prepared at 90% RH), and a freshly cleaved graphite surface. The statistics are obtained from scanning over 200 nm × 200 nm regions, similar to the conditions used in a previous study on graphene-on-mica [29]. The histograms are well fit by Gaussian distributions (solid lines). Standard deviations (σ) obtained from the Gaussian fits are listed in the figure. The measured surface roughness of mica and graphene on mica (27.3 and 23.4 pm) is similar to a previous study (34.3 and 24.1 pm).[29] On the other hand, the roughness of the graphite surface is measured to be considerably lower (13.5 pm vs. 22.6 pm), likely due to the differences in the specific settings of AFM. In general we find graphene on water adlayers has slightly lower surface roughness when compared to graphene on mica, which in turn is slightly smoother than the mica surface. These results suggest water molecules may be able to fill in surface defects on the atomic scale. However, as suggested in the previous study,[29] the measured roughness is likely limited by the noise of AFM.

In Figure 5.4 we present typical AFM images of graphene deposited on mica at ambient conditions [room temperature; relative humidity (RH) ~40%]. In agreement with a recent study,[29] we found graphene sheets spread atomically flat on mica over areas of 100-200 nm on a side (Figure 5.5). Over larger areas, however, island-like plateaus varying from a couple nanometers to a few micrometers in lateral size are observed across all the graphene samples (see also Figures 5.6, 5.8). These plateaus appear atomically flat (Figure 5.5), and plateaus from different samples have the same height of 0.37±0.02 nm (Figure 5.4, E and G), regardless of the lateral dimensions. Although dot-like thicker features are occasionally present, no plateaus with heights smaller than ~0.35 nm were observed.

The observed plateaus are not flakes of graphene or mica layers: such structures are not observed on the exfoliated surfaces of graphite and mica, or graphene deposited on SiO_2 substrates (Figure 5.6). In addition, the ~0.37 nm height is not consistent with the layer thicknesses of graphene (0.335 nm) or mica (0.99 nm), and, as described below, the structures themselves are dependent upon the relative humidity (RH) of the experimental conditions.

Figure 5.4FG presents data for the case in which the edge of a monolayer graphene sheet is folded underneath itself. A ~0.34 nm step height is observed for the folded graphene, while the same ~0.37 nm height is observed for plateaus both in and out of the folded region. Plateaus with the same height are also observed in bilayer graphene sheets, and the plateaus appear to be continuous across monolayer/bilayer borders (Figure 5.6). Our phase images further indicate that the plateau structures are under the graphene sheets (Figure 5.7). Plateau-like structures a few tenths of nms in height have been

noticed for multi-layer graphene on mica, and were also identified as gases or moisture trapped under graphene.[34] Indeed, albeit only one-atom thick, monolayer graphene is known to be robust and impermeable to liquid and gas.[35, 36]

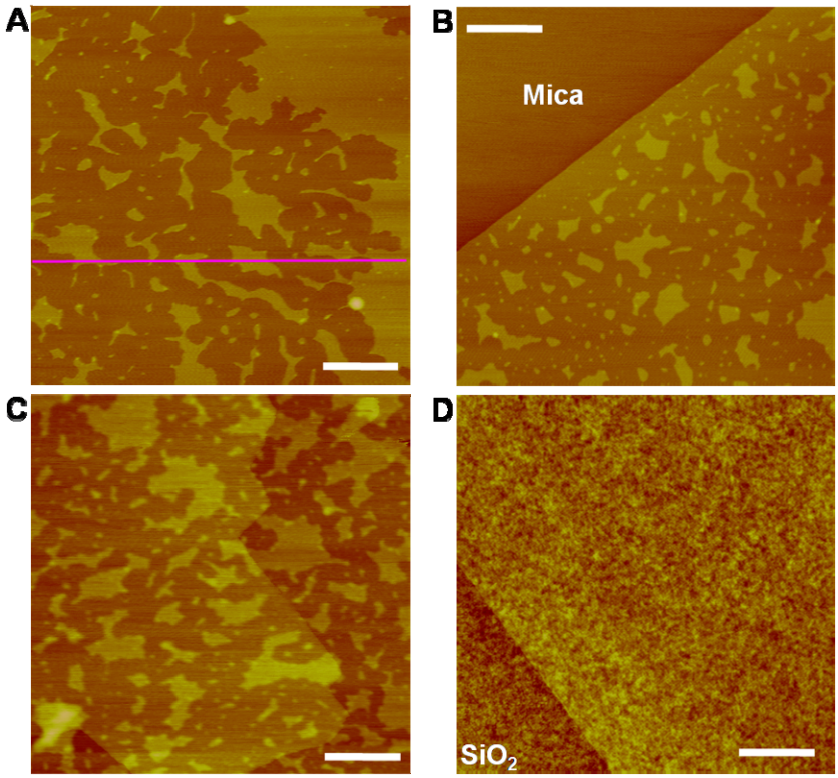

Figure 5.6. Additional AFM images of graphene deposited on mica and SiO_2 substrates under ambient conditions. (**A, B**) Additional images of monolayer graphene sheets deposited on mica. Pink line corresponds to the pink height profile in Figure 5.4E. (**C**) Image of another graphene-on-mica sample, at the border between bilayer (left) and monolayer (right) graphene sheets. (**D**) Image of a monolayer graphene sheet deposited on SiO_2 at ambient conditions. SiO_2 surfaces have very large surface roughness (standard deviations in height ~0.2 nm), and so adsorbed water molecules cannot form two-dimensional islands. Scale bars: 200 nm for (A) and (C). 500 nm for (B) and (D). The same height scale (4 nm) is used for all images.

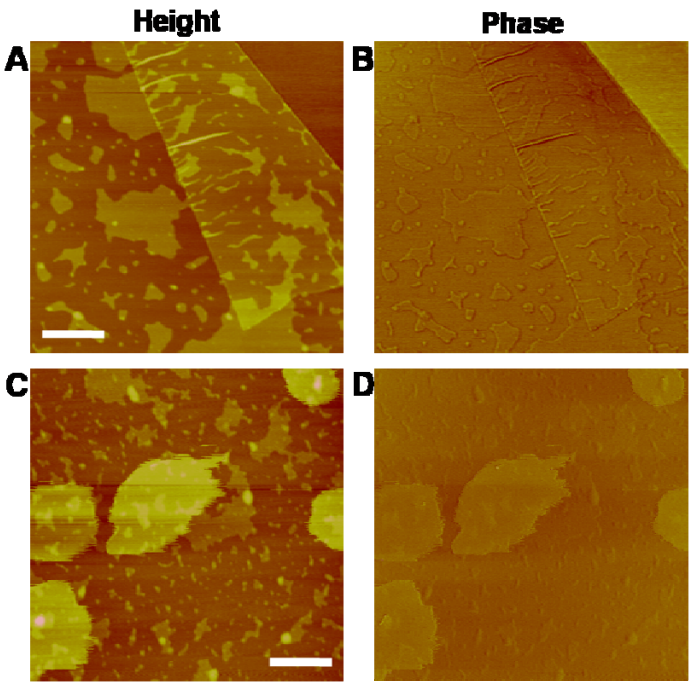

Figure 5.7. AFM phase images indicate the island-like plateau structures are under the graphene sheets. (**A**) Same as Figure 5.4F. The edge of the graphene sheet is folded underneath itself. (**B**) The corresponding phase image. Significant phase difference is observed between the mica (upper right corner) and graphene surfaces, reflecting the difference in surface properties.[37] In contrast, the same phase is observed for the plateaus and other parts of graphene (except for edges, which are always highlighted in phase images), indicating the AFM tip is interacting with the same surface (graphene), and the plateaus are underneath graphene. (**C**) AFM height image of a monolayer graphene sheet deposited on mica at ambient conditions, and then contaminated on the surface by the application of Scotch tape. (**D**) The corresponding phase image of (C). Contrasting phases are observed for the drop-like contaminants on the surface. On the other hand, the same phase is again observed for the plateaus and lower parts of graphene. In agreement with a recent study on friction force microscopy,[34] these results indicate the island-like plateau structures are under the graphene sheets. Scale bars: 200 nm. The same height scale (4 nm) is used for (A) and (C).

The observation of atomically flat plateaus that have well-defined heights and depend upon the RH indicates that the observed structures are not random gas molecules trapped between the graphene and mica surfaces, but instead are ordered water adlayers (Figure 5.4A). Previous SPFM studies have observed water layers on mica surfaces forming two-dimensional islands tens of nanometers to several microns in lateral size.[4, 13, 14] The shapes and size distribution of those water islands are in good agreement with the trapped structures in Figure 5.4, except that the presence of water islands smaller than a few tens of nanometers were not previously known, likely due to the ~10 nm lateral resolution of SPFM. The heights of the water islands were also not accurately determined with SPFM. The ~0.37 nm height we measured is in good agreement with the height of a monolayer of a "puckered bilayer" of ice ($c/2$ = 0.369 nm; Figure 5.4B),[33] a widely assumed model for how water molecules arrange in the first adlayer on a solid.[3, 6, 38]

We emphasize that although morphologically similar, the islands observed in the previous SPFM studies were the *second* water adlayer artificially induced on top of the first adlayer.[4, 14] The nature of the first adlayer was largely unknown due to the high mobility of water molecules at room temperature.[14] As will become more evident in the RH-dependent experiments (Figures 5.9 and 5.10), the plateaus we observed on samples prepared at ambient conditions (Figure 5.4) are the *first* water adlayer on the mica surface: the second adlayer only appears with high frequency at RH >~90%. For our case, graphene severs as an ultrathin coating and locks the first water adlayer into fixed patterns for AFM imaging.

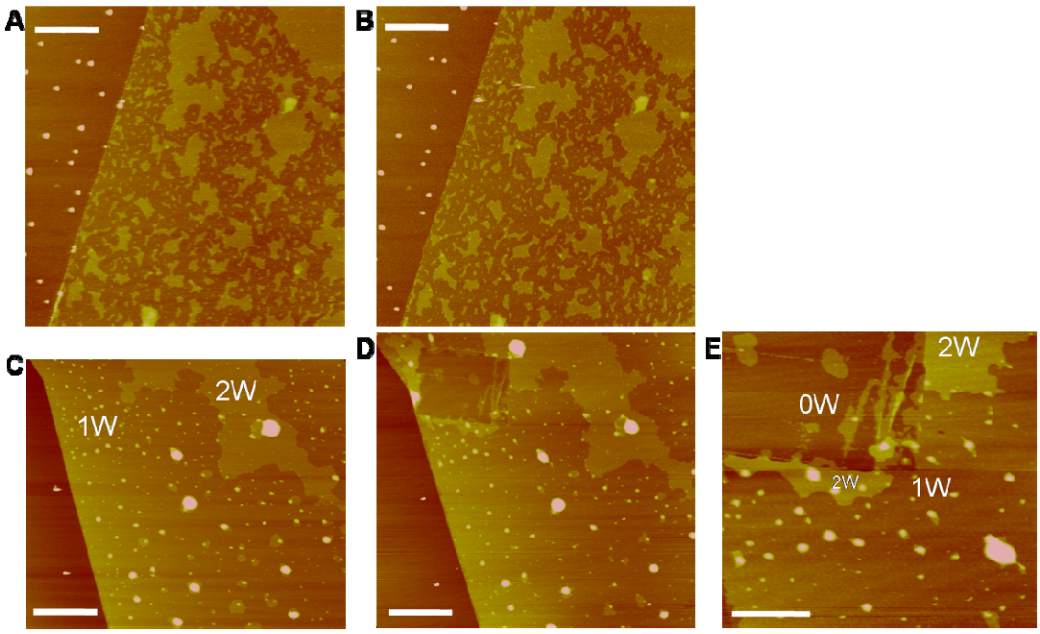

Figure 5.8. Stability of the graphene-fixed water patterns. (**A**) Another representative AFM image of a monolayer graphene sheet deposited on mica at ambient conditions. (**B**) The same sample, after being kept at ambient conditions for 25 days. No appreciable change of morphology is observed for the water patterns fixed by graphene. (**C**) An AFM image of monolayer graphene covering both the first (1W) and the second (2W) water adlayers on a mica substrate [from Figure 5.10D; realigned with Figure 5.8(D)]. (**D**) The same sample, after the entire mica substrate (~0.1 mm thick) was bent upwards by ~15 degrees. This excessive bending caused shear and partial displacement of graphene, and the water adlayer reorganized accordingly (upper left corner of the image). (**E**) A close-up of the change in (D). 0W, 1W, and 2W label the regions where graphene is on top of 0, 1, and 2 adlayers of water, respectively. During bending, water was squeezed out of a square ~1 μm in size and piled up at the edges of the square. Wrinkle-like features attributable to bending were also observed. Such square-like and wrinkle-like features are not observed in any samples that have not been subjected to extensive bending. Scale bars: 500 nm for (A), (B), and (E). 1 μm for (C) and (D). The same height scale (4 nm) is used for all images.

The fixed patterns are remarkably stable: besides preventing any appreciable changes of morphology during the several hours of our AFM operation, we found the patterns are stable for weeks under ambient conditions (Figure 5.8). We note, however, that the water adlayer can become mobile again when the mica substrate is subjected to extensive bending (Figure 5.8). Bending causes significant shear and displacement of graphene on the mica surface, thus releasing the locked water. The adlayer reorganizes accordingly, reflecting its dynamic nature.

The boundaries of the islands formed by the first water adlayer often exhibit fascinating polygonal shapes, with preferred angles of ~120°. For example, the arrow in Figure 5.4F points to an island with multiple 120° corners. This suggests at ambient conditions, the first water adlayer has an ice-like structure that is in epitaxial relationship with the substrate, similar to what was previously observed for the second water adlayer.[4, 13] This conclusion is further corroborated by the fact that all the islands have the same height as a single layer of ice, and is consonant with previous sum-frequency-generation spectroscopy results obtained over large areas.[8] The observed submonolayer coverage at ambient conditions is also consistent with previous macroscopic optical studies,[5, 7, 9] which indicated one statistical monolayer coverage at RH~75%, and a surface coverage of ~50% at RH~40%. In stark contrast to mica, graphitic surfaces (including graphene) are highly hydrophobic,[39, 40] and water is known to only adsorb on graphitic surfaces below ~150 K.[41] Therefore, in the sandwich structure (Figure 5.4A) no water is expected to come from the graphene side. The occasionally observed dot-like thicker features are possibly due to surface defects that attract water, as discussed below.

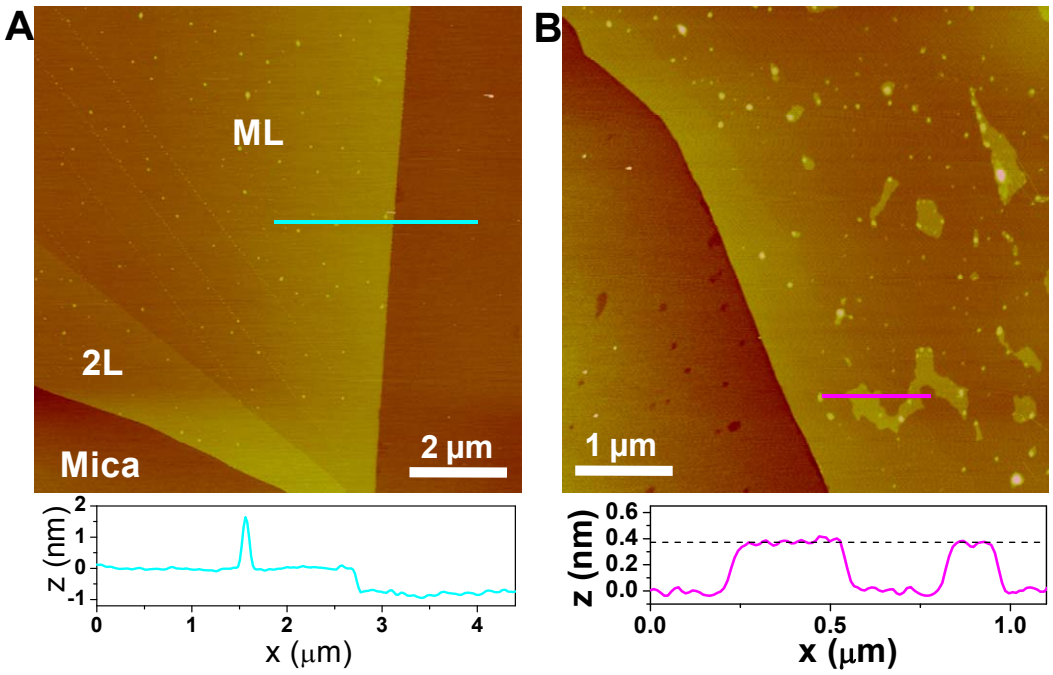

Figure 5.9. AFM images of graphene deposited on mica at RH ~2%, revealing the influence of surface defects on water adlayer nucleation. (**A**) A representative sample. ML: monolayer graphene. 2L: bilayer graphene. A dot-like defect is highlighted in the height profile across the cyan line. (**B**) Image of monolayer graphene deposited on a mica surface with high density of surface defects. A height profile is given for the pink line. The dash line indicates z = 0.37 nm. The same height scale (4 nm) is used for both images.

To investigate how the water adlayers evolve as the environmental humidity varies, we deposited graphene onto mica under controlled RH, and characterized the samples with AFM at ambient conditions. These studies also permitted investigations into the role that surface defects play in the initial formation of water adlayers. Figure 5.9A presents an AFM image of graphene deposited on mica under dry conditions (RH ~2%). No island-like structures are observed for most samples prepared in this way: graphene

lies atomically flat[29] (Figure 5.5) without observable features, except for sporadic dot-like structures ~2 nm in height, which are likely due to surface defects. This agrees with previous optical studies, which indicated[7, 9] no reliably detectable water adsorption on mica surfaces at RH~2%.

The measured height of monolayer graphene on bare mica surface is sensitive to the specific settings of AFM, and can vary from 0.4-0.9 nm. Similar height variations are observed for monolayer graphene on SiO_2 (0.5 to 1 nm),[31, 42] and are attributed to the large chemical contrast between graphene and the substrate.[31] This is why Raman spectroscopy provides such a useful probe for distinguishing graphene monolayers from bilayers and thicker films. The heights of the water islands in this study, however, can be accurately determined: the AFM tip is always interacting with the *same* material (graphene) that uniformly coats the underlying sample (Figure 5.4A); variations in tip-sample interactions are avoided.

Patchy islands are occasionally observed for graphene deposited at 2% RH, on mica surfaces that are characterized by a high density of surface defects (Figure 5.9B). The same height of ~0.37 nm is again measured for those islands, indicating a single adlayer of water. Interestingly, most islands connect nearby defects, suggesting the importance of defects for water adlayer nucleation. The adlayer boundaries appear round near the defect sites, but resume the 120° polygonal shape away from the defects, indicating a competition between capillary interactions and the epitaxial interactions with the substrate.

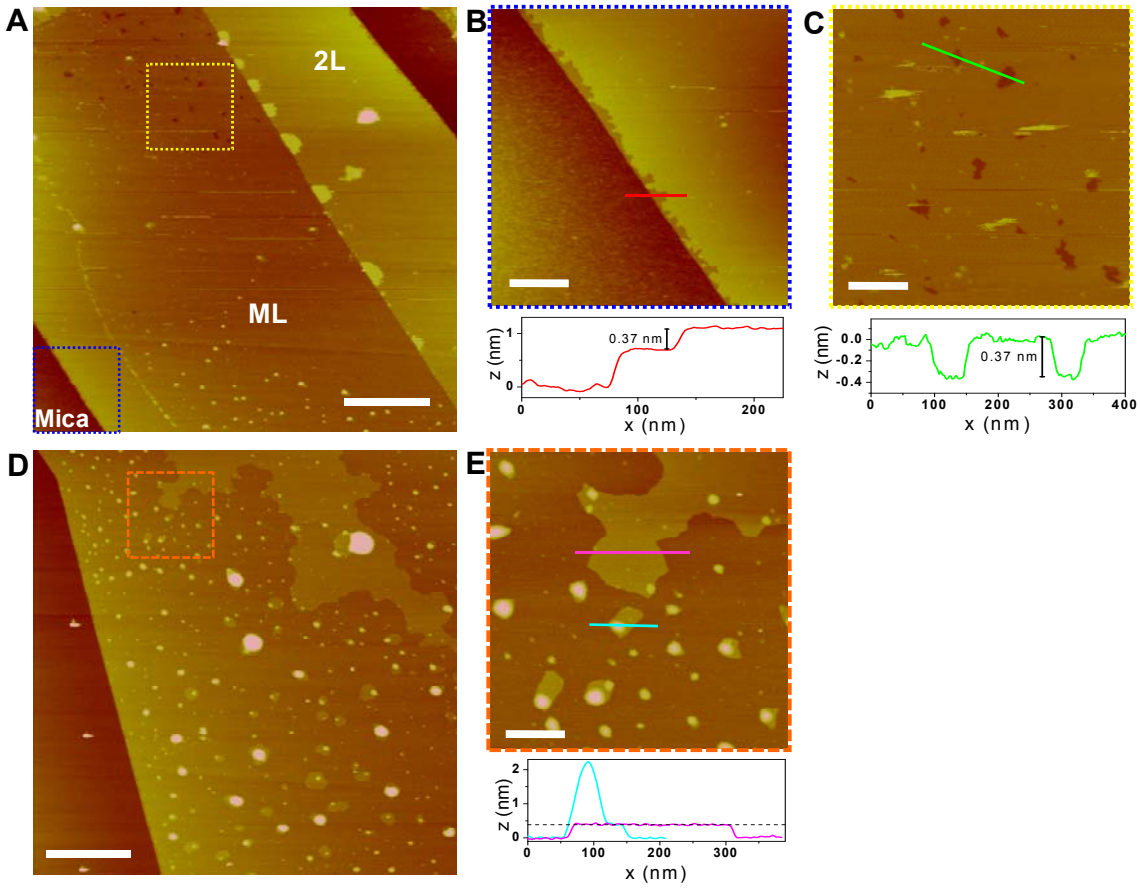

Figure 5.10. AFM images of graphene deposited on mica at RH ~90%, revealing the structure of the second water adlayer. (**A**) A representative sample. ML: monolayer graphene. 2L: bilayer graphene. (**B**) A close-up of the graphene edge, corresponding to the blue square at the bottom left of (A). A height profile is given for the red line. The first step (~0.7 nm in height) corresponds to monolayer graphene on bare mica. The second step (~0.37 nm) corresponds to the first water adlayer on mica, which has been sealed by the graphene. **(C)** A close-up of the pinholes, corresponding to the yellow square in (A). A height profile is given for the green line. (**D**) Image of monolayer graphene deposited on mica with a high density of surface defects. (**E**) A close-up of the *second* adlayer islands, corresponding to the orange square in (D). Height profiles are given for the pink and cyan lines. The dash line indicates z = 0.38 nm. Scale bars: 1 μm for (A) and (D), 200 nm for other images. The same height scale (4 nm) is used for all images.

When graphene is deposited on mica at high humidity (RH ~90%), the samples typically appear flat over large areas (Figure 5.10A). However, a closer look at the edge of the graphene sheets reveals that the graphene rides on top of a near-complete monolayer of water adlayer (Figure 5.10B). At about 10 nm from the edge of the graphene-water-mica sandwich structure, water evaporates away and graphene comes into direct contact with the mica surface, sealing and preserving the remaining water adlayers. The ~0.37 nm height (Figure 5.10B) indicates that the trapped water is a single adlayer. Polygonal pinholes ~10 nm in lateral size and ~0.37 nm in depth are also observed on the overall continuous adlayer (Figure 5.10C), indicating the monolayer is not 100% complete.

Different results are obtained for graphene deposited, at 90% RH, on a mica characterized by a high density of surface defects (Figure 5.10D). Besides a completed (no pinholes) first adlayer of water that is only missing at the graphene sheet edge, islands of various lateral sizes are observed on *top* of the first adlayer, often surrounding or connecting local defect sites. These islands are atomically flat (Figure 5.5), and are 0.38±0.02 nm in height over the first adlayer (Figure 5.10E), again in agreement with the height of a single "puckered bilayer" of ice (0.369 nm). The observed ~120° polygonal shapes of these islands agree with previous SPFM results on tip-induced second water adlayers.[4, 13, 14] Thus, the islands observed in Figure 5.10DE are the *second* water adlayer, which also has an ice-like structure at room temperature and is in epitaxial relationship with the first adlayer. Bulge-like features a few nanometers in height are also observed, but appear to be liquid-like (roundish) and have varying heights. No ice-like islands or plateaus were observed beyond the second adlayer. Previous optical studies[5, 7, 9] indicated

only a few statistical adlayers on the mica surface exist at RH~90%, but with large sample-to-sample variations - a result that is consistent with the observations reported here.

In summary, we find that graphene monolayers can provide an atomically flat surface coating that can enable measurements of the structures of the first water adlayers on mica at room temperature and at variable humidity. Under ambient conditions, water adlayers grow epitaxially on mica in a strictly layer-by-layer fashion: the second adlayer only forms after the first adlayer is fully completed. In the submonolayer regime, two-dimensional islands form due to interactions between adsorbed molecules, possibly akin to the Frank-van-der-Merwe growth mechanism in heteroepitaxy.[43] This result is consistent with previous studies that indicated the absence of dangling O-H bonds[8] and a minimum in entropy[9] at one statistical monolayer coverage. It also explains why water adsorption isotherms cannot be modeled with theories based on continuum models[7]. Our findings also highlight the role that surface defects play in water adsorption: defects apparently serve as nucleation centers for the formation of both the first and second adlayers. The importance of surface defects helps explain the large sample-to-sample variations previously reported in isotherm measurements.[5, 7] The use of STM[44-46] to characterize the atomic structures of graphene on water adlayers represents an exciting future challenge.

5.4 THF and cyclohexane on mica

Figure 5.11a shows a schematic of the graphene templating technique for investigating the structures of molecular layers of small organic molecules weakly adsorbed on the mica surface.

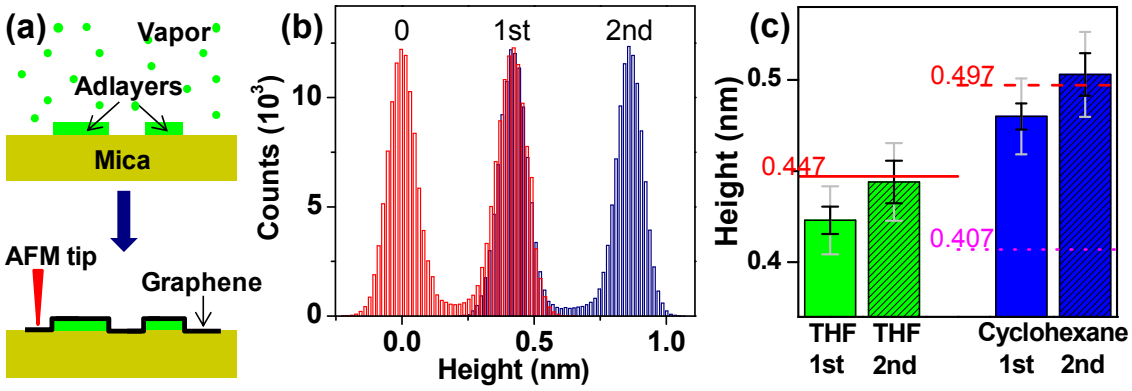

Figure 5.11. Graphene templating illustration (a) and representative measurements of adsorbed adlayer thicknesses (b,c). (b): Representative measurements of THF adlayer heights, from two AFM images, at the borders between 0 and 1 (red), and 1 and 2 (blue) adlayers. The two distributions are overlaid according to the peak centers of the first adlayer. The heights for the first and second adlayers are respectively determined to be 0.420 and 0.446 nm for the two specific samples. **(c)**: Statistics of the measured heights for the first and second adlayers of THF and cyclohexane on mica, obtained from ~10 samples for each adlayer. The indicated uncertainties (95% confidence) are for when the systematic error in height calibration is excluded (black) and included (grey). Red lines mark the known layer heights in the bulk crystals of THF (monoclinic) and cyclohexane (Phase I) that are in agreement with our data. The pink dotted line marks the layer height for a different crystal phase (Phase II) of cyclohexane crystal, and is in clear disagreement with our data.

Samples were prepared at room temperature (~22 °C) and a relative humidity of <2%, under which the adsorption of water on mica surfaces can be neglected.[1] Freshly cleaved mica surfaces were brought into contact with organic vapors and allowed to equilibrate for ~1 min. The partial pressure of organic molecules at the mica surface, which determines the surface coverage at equilibrium, was adjusted by varying the

distance between the vapor source and the mica. Graphene sheets were deposited onto the mica surface, sealing and preserving the adlayer structures. Samples were then removed from the organic vapors and imaged with AFM under ambient conditions.

Adlayer heights in each sample were determined by scanning over small (~200 nm) areas across adlayer borders, and plotting the distribution of all height values within the AFM images (Figure 5.11b). The final heights reported for THF and cyclohexane adlayers were summarized from the height values thus obtained from ~10 different images (Figure 5.11c).

Figure 5.12 presents typical AFM images of monolayer graphene sheets deposited on mica surfaces that were in equilibrium with THF vapors. Atomically flat islands/plateaus are observed across all graphene sheets. In comparison, no such structures are observed on mica surfaces that are not covered by graphene. Phase images,[1] which are more reflective of the local chemical properties of the surface rather than the topography,[37] indicate that the observed flat islands are THF adlayers trapped under the graphene, similar to the case of water adlayers in our previous study.[1] The numbers of THF adlayers, as labeled in Figure 5.12, were determined from measured heights and careful tracing of the extreme edges of graphene sheets, where the adlayers under graphene tend to evaporate away and leave the graphene in direct contact with the bare mica surface.[1]

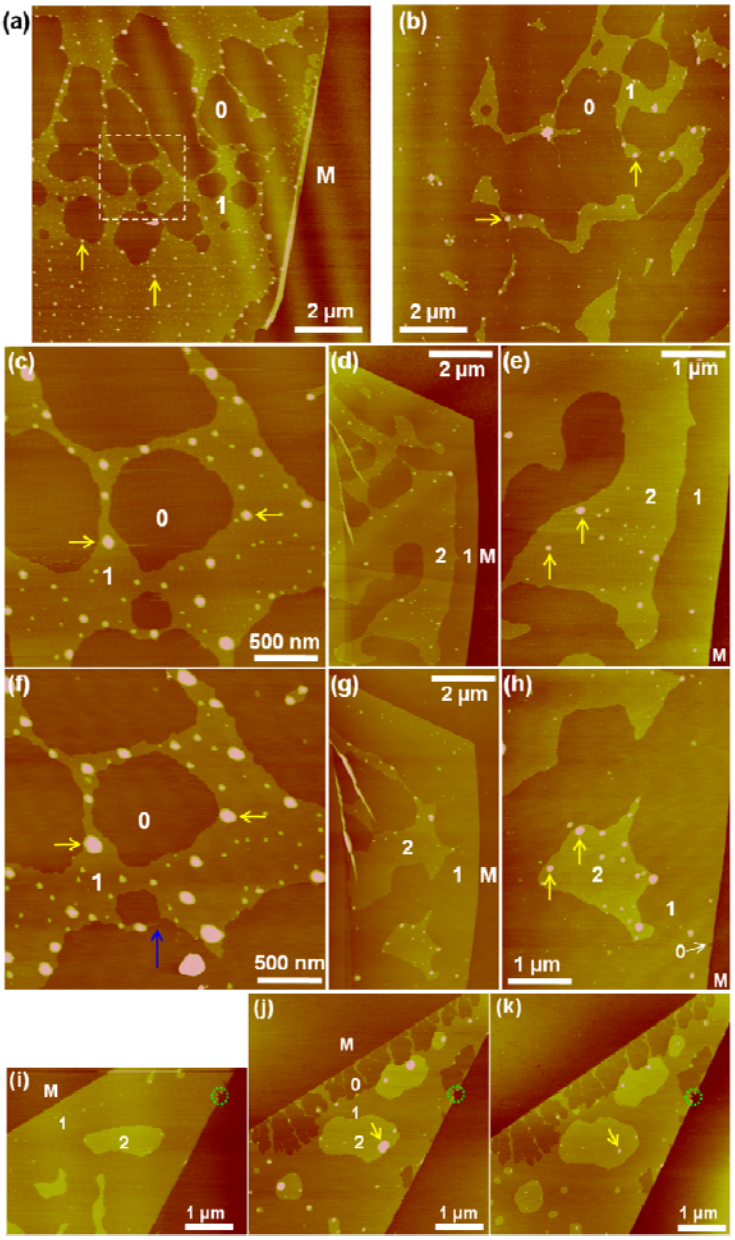

Figure 5.12. AFM images of graphene-templated THF adlayers reveal both structural and dynamical information. M labels the mica surface, and 0, 1 and 2 label regions where monolayer graphene is on top of 0, 1 and 2 adlayers of THF, respectively. Yellow arrows point to droplets. (a)-(e) were taken within a few hours after graphene sheets were deposited. **(a)**: The case in which the trapped adlayer is a submonolayer. **(b):** Another sample with very low surface coverage of THF. **(c):** Zoom-in of the square in (a). **(d):** Another sample showing the second THF adlayer on top of the first. **(e):** Zoom-in of the second adlayer in (d). **(f-h):** The same areas as (c-e), after the samples were kept at ambient conditions for 2 months. **(i-k):** Another sample freshly prepared (i), and after being kept at ambient conditions for 60 days (j) and 68 days (k). The green circles mark a defect on the graphene edge, which served as a reference point for aligning the images.

Interestingly, similar to what was found for water,[1] a layer-by-layer growth mechanism is observed for the first two adlayers of THF molecules: the second adlayer only forms after the first adlayer is completed (Figure 5.12de), and two-dimensional (2D) flat islands are observed for both layers, similar to the Frank-van-der-Merwe growth mechanism in heteroepitaxy.[43] No molecularly flat, island-like structures are seen beyond the second adlayer; droplets are observed to coexist with both the first and second adlayers. This general mechanism, however, is not universal: it can be altered by chemical modification of the mica surface. For example, very different behavior is observed for water adlayers adsorbed on trimethylchlorosilane-functionalized (somewhat hydrophobic; H_2O contact angle ~ 40^o) mica. The adlayer structures that initially adsorb, as observed via graphene templating, are three-dimensional nanodroplets only, with no obvious crystalline structure (Figure 5.13). Those results indicate multiple types of adlayer growth mechanisms can be achieved via chemical modification of the underlying mica substrate, and can be preserved and imaged using graphene templating.

Figure 5.12a-c present the case in which the trapped adlayer is a submonolayer. Large, interconnecting islands coexist with areas where no adlayer is present. At low surface coverage, the adlayers tend to form narrow "necks" as opposed to isolated small islands (Figure 5.12b). This contrasts with what is seen for submonolayers of water, where isolated and scattered small islands, typically ~10 nm in lateral size, are observed[1] (see also Figure 5.8). This result suggests that, relative to water, THF molecules interact more weakly with the mica surface, so the interactions between THF molecules dominate and lead to more continuous adlayers.

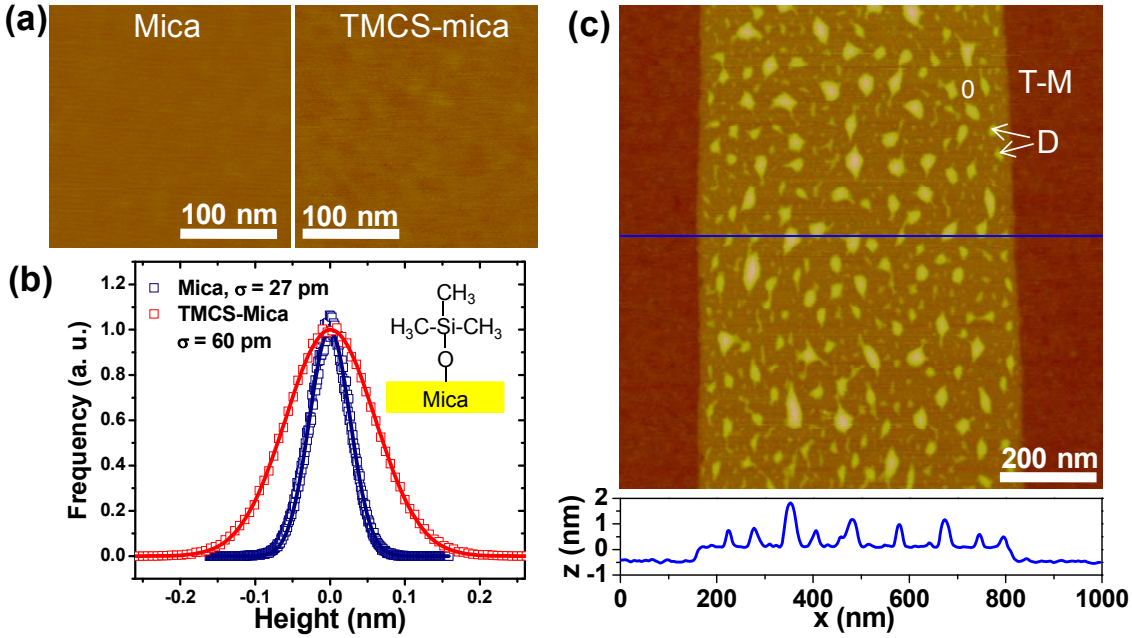

Figure 5.13. Water adsorption on TMCS-functionalized mica surfaces at ambient conditions. (a): AFM images indicate a uniform surface passivation of mica by TMCS. However, the functionalized surface, although still very flat, is rougher than what is observed for freshly cleaved mica. **(b):** Height histograms of a fresh mica surface and a TMCS-functionalized mica surface. The measured RMS roughness of fresh mica (27 pm) is likely limited by the noise of AFM, whereas the roughness of TMCS-functionalized mica surface is significantly higher (60 pm). There is, however, no evidence that TMCS functionalization introduces etch pits or other large defects into the mica. The inset is a simple molecular drawing of TMCS-functionalized mica. **(c):** Graphene-templating reveals that under ambient conditions (~40% RH), water adsorbs as nanometer-sized droplets on the relatively hydrophobic TMCS-functionalized mica surface. "T-M" labels TMCS-functionalized mica surface, "0" labels where monolayer graphene is in direct contact with the TMCS-functionalized mica surface, and "D" points to two droplets. A cross-sectional profile is given for the blue line, which indicates the droplets have varying heights on the order of ~1-2 nm. These results contrast with the flat 2D islands typically observed for adlayers on fresh (hydrophilic) mica surfaces.

The boundaries of the islands formed by the first THF adlayers often appear rounded (Figure 5.12a-c). Similar rounded boundaries are also observed at the missing edges of full monolayers (not shown here). These results suggest that the first THF adlayer has at least some liquid-like characteristics. The second adlayers (Figure 5.12de), on the other hand, exhibit both rounded and faceted boundaries. As will be discussed below, the rounded boundaries of THF adlayers become increasingly faceted over time scales of weeks, suggesting, again, that these adlayers possess both liquid and solid properties at room temperature. These results also contrast with water, for which both the first and second adlayers appear ice-like at room temperature, and are characterized by faceted boundaries with preferred angles of ~120°.[1, 4, 13]

The heights of the first and second THF adlayers on the mica surface were measured, across ~10 samples, to be 0.42±0.02 and 0.44±0.02 nm, respectively (95% confidence; Figure 5.11c). The height of the second adlayer is in good agreement with the layer thickness in THF crystals: THF crystallizes in the monoclinic space group $C2/c$, and the layer thickness in the b direction is $b/2$ = 0.447 nm (Figure 5.11c).[47-49] In this direction, THF molecules "stand up" with the oxygen atoms in the rings alternatively pointing towards and away from the substrate.[49] This also corresponds to the polarity direction for THF molecules. The height of the first adlayer is statistically thinner than the second adlayer: when the (systematic) uncertainty in height calibration is ignored, the heights of the first and second THF adlayers can be expressed as 0.423±0.008 and 0.444±0.012 nm, respectively. This result suggests the first THF adlayer may be slightly thinner than the layer thickness in the crystal (Figure 5.11c), possibly indicating that the

first adlayers are slightly tilted due to interactions with the substrate (Figure 5.15ab), a phenomenon often encountered in self-assembled monolayers on substrates.[50]

Although the graphene-templated THF adlayers are stable over time scales of hours (e.g., the same structures are observed for images taken at different magnifications over periods of several hours), noticeable structural changes are observed over the time scale of weeks. This result is in contrast to graphene-templated water adlayers, which are stable for at least months under ambient conditions (Figure 5.8).[1] In most cases, the THF adlayers shrink in lateral dimensions to form droplets (Figure 5.12f-h). Narrow "necks" in the adlayers thus tend to break (blue arrow in Figure 5.12f). The boundaries of the THF adlayers also often adopt facets during the reorganization (Figure 5.12f-h). These observations are reminiscent of the coalescence of molecularly thin clusters/islands often encountered during the post-deposition relaxation processes in thin film deposition.[51-53] In our case, adlayers are sealed under graphene, so the vapor-adlayer equilibrium is removed for the otherwise volatile molecules. The adlayers thus relax in a manner that is similar to deposited nonvolatile thin films. We further note that after the adlayers are allowed to relax for sufficiently long periods (Figure 5.12ij); reverse processes, in which droplets shrink in size to form larger adlayer islands, are also occasionally observed (Figure 5.12k). Such reversible island-droplet-island transitions are likely due to thermal fluctuations, and are consistent with the idea that all of the adlayer structures observed here are within a few k_BT of energy.

The observations on the THF adlayers imply both liquid-like and crystalline characteristics at room temperature. This is remarkable since room temperature is ~130 K higher than the bulk melting point of THF (-108.4 °C). The coexistence of solid-like and

liquid-like layers have been recently observed for the ionic liquid Bmim-PF_6 on mica surfaces.[54] However, the melting point of Bmim-PF_6 (6.6 °C) is close to room temperature, and the liquid-like and solid-like structures observed in Bmim-PF_6 films, which are of unknown thicknesses,[54] likely only reflect the differences between bulk and adlayer properties. The faceted yet mobile adlayers we observed have not been previously reported. One possible explanation of our result is that the THF adlayers are in a "hexatic" phase that is between the solid and liquid phases. In three dimensions, liquid-solid transitions are necessarily first-ordered and abrupt; for 2D systems the liquid-solid transition may occur continuously, through the intermediate "hexatic" phase, and over a wide temperature range.[55-57]

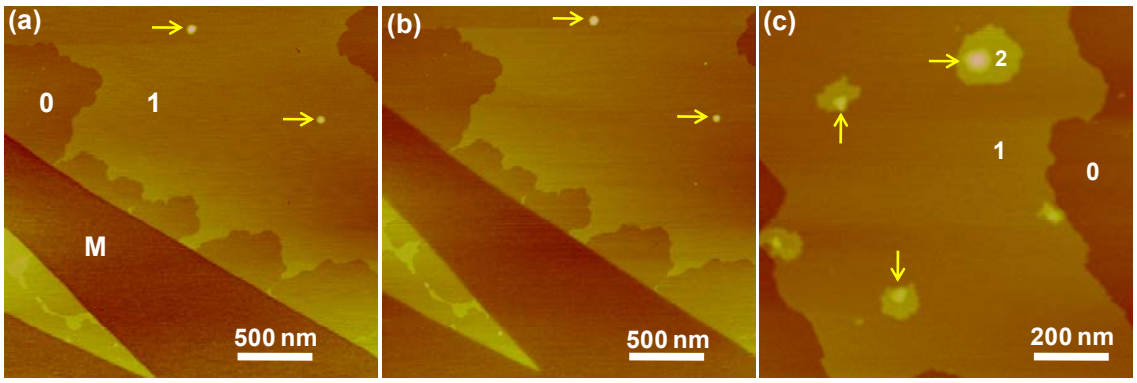

Figure 5.14. AFM images of graphene-templated cyclohexane adlayers. M labels the mica surface, and 0, 1 and 2 label regions where monolayer graphene is on top of 0, 1, and 2 adlayers of cyclohexane, respectively. Yellow arrows point to droplets. **(a):** A typical image of graphene-templated submonolayer cyclohexane adlayer, taken within a few hours after graphene was deposited. **(b):** The same area, but imaged after the sample was stored at ambient conditions for 2 months. **(c):** Another sample showing the second cyclohexane adlayers.

Figure 5.14 presents typical AFM images of monolayer graphene deposited on mica surfaces that were in equilibrium with cyclohexane vapors at room temperature. Similar to the case of both water and THF adlayers, a layer-by-layer growth mechanism is generally observed for cyclohexane adlayers, and atomically flat 2D islands are observed for both the first and the second adlayers. The surface coverage of cyclohexane on the mica surface is usually low, and so the second adlayer was only occasionally observed, typically surrounding droplets that are likely attracted by surface defects (Figure 5.14c). This result possibly reflects the weaker interaction between the non-polar cyclohexane molecules and the mica surface.

Similar to the case of THF, but different from water, cyclohexane adlayers form large, continuous islands on mica, indicating weak molecule-substrate interactions. On the other hand, similar to the case of water but different from THF, the boundaries of all cyclohexane adlayers appear faceted, suggesting the adlayers are crystal-like at room temperature. In addition, under ambient conditions the graphene-templated cyclohexane adlayers are found to be stable for months without noticeable structural changes (Figure 5.14b), again indicating that the adlayers are solid-like at room temperature, similar to the case of water adlayers (Figure 5.8). The crystallinity of the cyclohexane adlayers, relative to THF adlayers, is likely due to the large difference in melting points (6.7 ^{o}C vs. -108.4 ^{o}C), and suggests that the interaction between adsorbed molecules plays an important role in determining the adlayer structure.

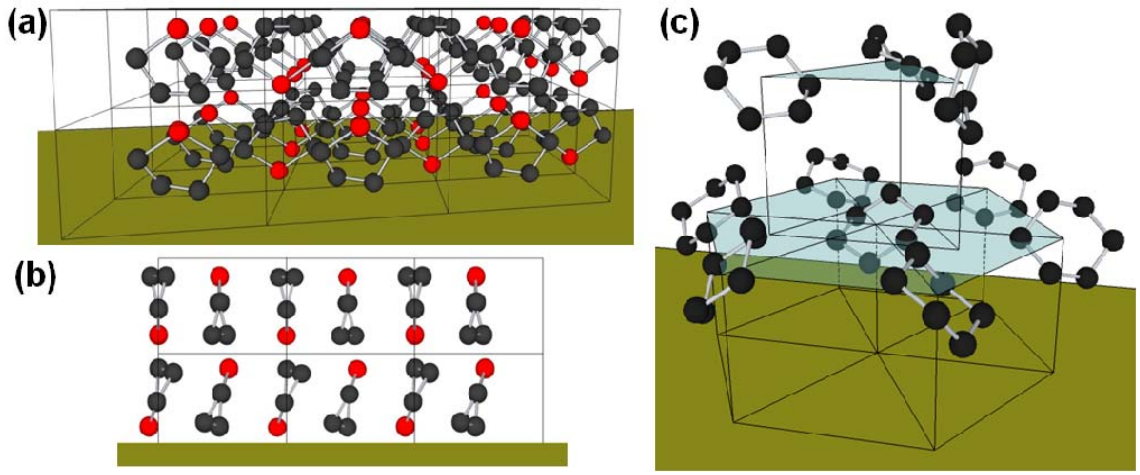

Figure 5.15. Possible structural models for THF and cyclohexane adlayers. Black and red balls represent carbon and oxygen atoms, respectively. Hydrogen atoms are omitted for clarity. **(a,b):** Possible structure of the first two adlayers of THF, basing on the monoclinic crystal structure of THF. (a): Perspective view. (b): Side view. The first adlayer may be tilted due to molecule-substrate interactions. **(c):** Instantaneous view of the possible structure of the first two adlayers of cyclohexane. The structure is based on the (111) direction of the fcc lattice of the Phase I "plastic crystal" structure of cyclohexane. Each molecule is free to rotate about its center, and so this view represents one instantaneous snapshot. The rotational freedom may be lower for the first adlayer.

The heights of the first and second cyclohexane adlayers on the mica surface, across different samples, are measured to be 0.48±0.02 and 0.50±0.02 nm, respectively (Figure 5.11c). These values are in good agreement with the layer thickness of the Phase I crystal structure of cyclohexane. Phase I is the stable phase for bulk cyclohexane between 279.8 K and 186 K. The unit cell is face-center cubic (fcc) with a = 0.861 nm.[58, 59] The layer thickness in the (111) direction (i.e., a close-packed hexagonal single layer; Figure 5.15c) is thus $a/\sqrt{3}$ ~0.497 nm (Figure 5.11c). Previous low-energy electron

diffraction (LEED) studies[26, 27] over large areas of cyclohexane adlayers on Pt(111) and Ag(111) surfaces indicated that for T <~200 K, cyclohexane adsorbs as a monoclinic phase, which is consistent with the Phase II crystal structure. That structure is known to be stable for T < 186 K in bulk. According to the Phase II arrangement, the cyclohexane rings would lie roughly parallel to the substrate,[26, 27] and the layer thickness should be ~c/2 sinβ = 0.407 nm.[58] That value is significantly smaller than the adlayer heights we measured (Figure 5.11c). No LEED patterns were observed in previous studies for T >~200 K, where cyclohexane adlayers evaporated in vacuum.[26, 27] Thus, our results suggest at room temperature, cyclohexane adlayers crystallize as Phase I (Figure 5.15c). Phase I of cyclohexane is plastic crystal, meaning that although molecules form ordered crystal lattices, they are still free to rotate about the lattice points.[58, 59] The layer height is larger than for the case of Phase II, in which all molecules lie "flat" on substrate. Similar to the case of THF, and neglecting the systematic uncertainty in height calibration, the height of the first adlayer of cyclohexane (0.480±0.007) is statistically thinner than the second adlayer (0.503±0.012 nm) (Figure 5.11c). One possibility is that interactions with the substrate may restrain the rotation of first adlayer cyclohexane molecules on the mica surface (Figure 5.15c).

We have reported on the room-temperature structures and dynamics of weakly bound adlayers at the interfaces between solids and vapors of small organic molecules by using graphene templating. We found cyclohexane adlayers on mica are crystal-like at room temperature, whereas THF adlayers possess both liquid and solid properties. The heights of the second adlayers of THF and cyclohexane are in agreement with the layer thicknesses in the monoclinic crystal structure of THF and the Phase I "plastic crystal"

structure of cyclohexane. The first adlayers of both molecules appear slightly thinner, indicative of molecule/mica interactions. A layer-by-layer growth mechanism has so far been consistently observed for the first two adlayers of water, THF, and cyclohexane molecules on freshly cleaved mica. Previous studies indicated that for nonvolatile, large organic molecules, layer-by-layer spreading also occurs on flat substrates, both for molecules that are solid[21, 23, 24] and liquid[19, 20, 54] at room temperature. The striking consistency and similarity across different systems suggest that the layer-by-layer mechanism may be broadly applicable for molecular adsorbates on many atomically flat surfaces, although more experiments are required to validate this hypothesis.

An outstanding question involves the influence that the graphene exerts on the adlayer structure. All of our findings to date indicate that graphene templating permits unprecedented high-resolution views of weakly bound molecular adlayers, and the resultant data is wholly consistent with previous findings. This indicates that, at least for some systems, graphene templating provides a relatively innocent structural probe. However, it is likely that detailed quantum mechanical calculations will be required to more fully address this question, and that the answer will be system-dependent.

5.5 Conclusion

In this chapter, graphene templating is utilized to visualize the first adlayers of water and small organic molecules (THF and cyclohexane) on mica at ambient conditions, revealing how the atomic structure of the adlayers evolves at the nanometer/molecular scale.

Due to its dynamic nature, the room-temperature microscopic structure of the first water adlayers on solid surfaces has been challenging to detect. By employing graphene as an atomically flat coating for atomic force microscopy, we measured the structure of the water adlayers on mica at room temperature, and as a function of relative humidity. We found that water adlayers grow epitaxially on the mica substrate in a layer-by-layer fashion. Submonolayers form atomically flat, faceted islands of height 0.37±0.02 nm, in agreement with the height of a monolayer of ice. The second adlayers, observed at higher relative humidity, also appear ice-like, and thicker layers appear liquid-like. Our results also indicate nanometer-scale surface defects serve as nucleation centers for the formation of both the first and second adlayers.

In the remainder of the chapter, we report on the use of graphene templating to investigate the room-temperature structure and dynamics of weakly bound adlayers at the interfaces between solids and vapors of small organic molecules. Monolayer graphene sheets are employed to preserve and template molecularly thin adlayers of tetrahydrofuran (THF) and cyclohexane on atomically flat mica substrates, thus permitting a structural characterization of the adlayers under ambient conditions through atomic force microscopy. We found the first two adlayers of both molecules adsorb in a layer-by-layer fashion, and atomically flat two-dimensional islands are observed for both the first and the second adlayers. THF adlayers form initially as rounded islands, but over a time period of weeks evolve into faceted islands, suggesting that the adlayers possess both liquid and solid properties at room temperature. Cyclohexane adlayers form crystal-like faceted islands, and are immobile under the graphene template. Precise adlayer height measurements further permitted the identification of the crystal structures of the

adlayers. The heights of the second adlayers of THF and cyclohexane are measured to be 0.44±0.02 and 0.50±0.02 nm, respectively, in good agreement with the layer thicknesses in the monoclinic crystal structure of THF and the Phase I "plastic crystal" structure of cyclohexane. The first adlayers appear slightly thinner for both molecules, indicative of interactions of the molecules with the mica substrate.

5.6 References

1. Xu, K., Cao, P.G. & Heath, J.R. Graphene visualizes the first water adlayers on mica at ambient conditions. *Science* **329**, 1188-1191 (2010).
2. Cao, P.G., Xu, K., Varghese, J.O. & Heath, J.R. Atomic force microscopy characterization of room-temperature adlayers of small organic molecules through graphene templating. *J Am Chem Soc* **133**, 2334-2337 (2011).
3. Thiel, P.A. & Madey, T.E. The interaction of water with solid-surfaces: fundamental aspects. *Surf. Sci. Rep.* **7**, 211-385 (1987).
4. Verdaguer, A., Sacha, G.M., Bluhm, H. & Salmeron, M. Molecular structure of water at interfaces: Wetting at the nanometer scale. *Chem Rev* **106**, 1478-1510 (2006).
5. Ewing, G.E. Ambient thin film water on insulator surfaces. *Chem Rev* **106**, 1511-1526 (2006).
6. Feibelman, P.J. The first wetting layer on a solid. *Phys. Today* **63(2)**, 34-39 (2010).
7. Beaglehole, D., Radlinska, E.Z., Ninham, B.W. & Christenson, H.K. Inadequacy of Lifshitz theory for thin liquid-films. *Phys Rev Lett* **66**, 2084-2087 (1991).
8. Miranda, P.B., Xu, L., Shen, Y.R. & Salmeron, M. Icelike water monolayer adsorbed on mica at room temperature. *Phys Rev Lett* **81**, 5876-5879 (1998).
9. Cantrell, W. & Ewing, G.E. Thin film water on muscovite mica. *J Phys Chem B* **105**, 5434-5439 (2001).
10. Bluhm, H. & Salmeron, M. Growth of nanometer thin ice films from water vapor studied using scanning polarization force microscopy. *J. Chem. Phys.* **111**, 6947-6954 (1999).
11. Ogawa, K. & Majumdar, A. Molecular-level imaging of ice crystal structure and dynamics by atomic force microscopy. *Microscale Thermophys. Eng.* **3**, 101-110 (1999).
12. Piner, R.D. & Mirkin, C.A. Effect of water on lateral force microscopy in air. *Langmuir* **13**, 6864-6868 (1997).

13. Hu, J., Xiao, X.D., Ogletree, D.F. & Salmeron, M. Imaging the condensation and evaporation of molecularly thin-films of water with nanometer resolution. *Science* **268**, 267-269 (1995).

14. Xu, L. & Salmeron, M. in Nano-Surface Chemistry. (ed. M. Rosoff) 243-287 (Marcel Dekker, New York; 2001).

15. Weaver, J.F., Carlsson, A.F. & Madix, R.J. The adsorption and reaction of low molecular weight alkanes on metallic single crystal surfaces. *Surf. Sci. Rep.* **50**, 107-199 (2003).

16. Goss, K.U. The air/surface adsorption equilibrium of organic compounds under ambient conditions. *Crit. Rev. Environ. Sci. Technol.* **34**, 339-389 (2004).

17. Bruch, L.W., Diehl, R.D. & Venables, J.A. Progress in the measurement and modeling of physisorbed layers. *Rev. Mod. Phys.* **79**, 1381-1454 (2007).

18. Beaglehole, D. & Christenson, H.K. Vapor adsorption on mica and silicon - entropy effects, layering, and surface forces. *J. Phys. Chem.* **96**, 3395-3403 (1992).

19. Xu, L., Salmeron, M. & Bardon, S. Wetting and molecular orientation of 8CB on silicon substrates. *Phys Rev Lett* **84**, 1519-1522 (2000).

20. Xu, L. et al. De-wetting of lubricants on hard disks. *J. Chem. Phys.* **112**, 2952-2957 (2000).

21. Lazar, P., Schollmeyer, H. & Riegler, H. Spreading and two-dimensional mobility of long-chain alkanes at solid/gas interfaces. *Phys Rev Lett* **94**, 116101 (2005).

22. Riegler, H. & Kohler, R. How pre-melting on surrounding interfaces broadens solid-liquid phase transitions. *Nat. Phys.* **3**, 890-894 (2007).

23. Trogisch, S. et al. Atomic force microscopy measurements of topography and friction on dotriacontane films adsorbed on a SiO_2 surface. *J. Chem. Phys.* **123**, 154703 (2005).

24. Cisternas, E.A. et al. Crystalline-to-plastic phase transitions in molecularly thin n-dotriacontane films adsorbed on solid surfaces. *J. Chem. Phys.* **131**, 114705 (2009).

25. Giancarlo, L.C. & Flynn, G.W. Scanning tunneling and atomic force microscopy probes of self-assembled, physisorbed monolayers: peeking at the peaks. *Annu Rev Phys Chem* **49**, 297-336 (1998).

26. Firment, L.E. & Somorjai, G.A. Surface-structures of normal paraffins and cyclohexane monolayers and thin crystals grown on (111) crystal-face of platinum - low-energy electron-diffraction study. *J. Chem. Phys.* **66**, 2901-2913 (1977).

27. Firment, L.E. & Somorjai, G.A. Low-energy electron-diffraction study of surface of thin crystals and monolayers of normal paraffins and cyclohexane on Ag(111) crystal-surface. *J. Chem. Phys.* **69**, 3940-3952 (1978).

28. Novoselov, K.S. et al. Two-dimensional atomic crystals. *Proc. Natl. Acad. Sci. U. S. A.* **102**, 10451-10453 (2005).
29. Lui, C.H., Liu, L., Mak, K.F., Flynn, G.W. & Heinz, T.F. Ultraflat graphene. *Nature* **462**, 339-341 (2009).
30. Nair, R.R. et al. Fine structure constant defines visual transparency of graphene. *Science* **320**, 1308-1308 (2008).
31. Ferrari, A.C. et al. Raman spectrum of graphene and graphene layers. *Phys Rev Lett* **97**, 187401 (2006).
32. Graf, D. et al. Spatially resolved Raman spectroscopy of single- and few-layer graphene. *Nano Lett.* **7**, 238-242 (2007).
33. Fletcher, N.H. The chemical physics of ice. (Cambridge Univ. Press, London; 1970).
34. Lee, C. et al. Frictional characteristics of atomically thin sheets. *Science* **328**, 76-80 (2010).
35. Bunch, J.S. et al. Impermeable atomic membranes from graphene sheets. *Nano Lett.* **8**, 2458-2462 (2008).
36. Stolyarova, E. et al. Observation of graphene bubbles and effective mass transport under graphene films. *Nano Lett.* **9**, 332-337 (2009).
37. Garcia, R. & Perez, R. Dynamic atomic force microscopy methods. *Surf. Sci. Rep.* **47**, 197-301 (2002).
38. Doering, D.L. & Madey, T.E. The adsorption of water on clean and oxygen-dosed Ru(001). *Surf Sci* **123**, 305-337 (1982).
39. Leenaerts, O., Partoens, B. & Peeters, F.M. Water on graphene: hydrophobicity and dipole moment using density functional theory. *Phys Rev B* **79**, 235440 (2009).
40. Shin, Y.J. et al. Surface-energy engineering of graphene. *Langmuir* **26**, 3798-3802 (2010).
41. Bolina, A.S., Wolff, A.J. & Brown, W.A. Reflection absorption infrared spectroscopy and temperature-programmed desorption studies of the adsorption and desorption of amorphous and crystalline water on a graphite surface. *J Phys Chem B* **109**, 16836-16845 (2005).
42. Novoselov, K.S. et al. Electric field effect in atomically thin carbon films. *Science* **306**, 666-669 (2004).
43. Herman, M.A., Richter, W. & Sitter, H. Epitaxy: physical principles and technical implementation. (Springer, Berlin; 2004).
44. Ishigami, M., Chen, J.H., Cullen, W.G., Fuhrer, M.S. & Williams, E.D. Atomic structure of graphene on SiO_2. *Nano Lett.* **7**, 1643-1648 (2007).

45. Stolyarova, E. et al. High-resolution scanning tunneling microscopy imaging of mesoscopic graphene sheets on an insulating surface. *Proc. Natl. Acad. Sci. U. S. A.* **104**, 9209-9212 (2007).

46. Xu, K., Cao, P.G. & Heath, J.R. Scanning tunneling microscopy characterization of the electrical properties of wrinkles in exfoliated graphene monolayers. *Nano Lett.* **9**, 4446-4451 (2009).

47. David, W.I.F. & Ibberson, R.M. A reinvestigation of the structure of tetrahydrofuran by high-resolution neutron powder diffraction. *Acta Crystallogr. Sect. C-Cryst. Struct. Commun.* **48**, 301-303 (1992).

48. Luger, P. & Buschmann, J. Twist conformation of tetrahydrofuran in the crystal. *Angew. Chem.-Int. Edit. Engl.* **22**, 410-410 (1983).

49. Dziubek, K.F., Jeczminski, D. & Katrusiak, A. Pressure-generated hydrogen bonds and the role of subtle molecular features in tetrahydrofuran. *J. Phys. Chem. Lett.* **1**, 844-849 (2010).

50. Ulman, A. Formation and structure of self-assembled monolayers. *Chem Rev* **96**, 1533-1554 (1996).

51. Zinkeallmang, M., Feldman, L.C. & Grabow, M.H. Clustering on surfaces. *Surf. Sci. Rep.* **16**, 377-463 (1992).

52. Venables, J.A., Spiller, G.D.T. & Hanbucken, M. Nucleation and growth of thin-films. *Rep. Prog. Phys.* **47**, 399-459 (1984).

53. Evans, J.W., Thiel, P.A. & Bartelt, M.C. Morphological evolution during epitaxial thin film growth: Formation of 2D islands and 3D mounds. *Surf. Sci. Rep.* **61**, 1-128 (2006).

54. Liu, Y.D., Zhang, Y., Wu, G.Z. & Hu, J. Coexistence of liquid and solid phases of Bmim-PF_6 ionic liquid on mica surfaces at room temperature. *J Am Chem Soc* **128**, 7456-7457 (2006).

55. Strandburg, K.J. Two-dimensional melting. *Rev. Mod. Phys.* **60**, 161-207 (1988).

56. Binder, K., Sengupta, S. & Nielaba, P. The liquid-solid transition of hard discs: first-order transition or Kosterlitz-Thouless-Halperin-Nelson-Young scenario? *J. Phys.-Condes. Matter* **14**, 2323-2333 (2002).

57. Gasser, U., Eisenmann, C., Maret, G. & Keim, P. Melting of crystals in two dimensions. *ChemPhysChem* **11**, 963-970 (2010).

58. Kahn, R., Fourme, R., Andre, D. & Renaud, M. Crystal structures of cyclohexane I and II. *Acta Crystallogr. Sect. B-Struct. Commun.* **B 29**, 131-138 (1973).

59. Shigematsu, K., Hondo, H., Kumagai, T. & Takahashi, Y. Pressure effect on the solid I-liquid and solid III-solid I equilibrium forms of cyclohexane. *Cryst. Growth Des.* **9**, 4674-4679 (2009).